

Decay of dipolar vortex structures in a stratified fluid

Citation for published version (APA):

Flór, J-B., Heijst, van, G. J. F., & Delfos, R. (1995). Decay of dipolar vortex structures in a stratified fluid. *Physics of Fluids*, 7(2), 374-383. <https://doi.org/10.1063/1.868635>

DOI:

[10.1063/1.868635](https://doi.org/10.1063/1.868635)

Document status and date:

Published: 01/01/1995

Document Version:

Publisher's PDF, also known as Version of Record (includes final page, issue and volume numbers)

Please check the document version of this publication:

- A submitted manuscript is the version of the article upon submission and before peer-review. There can be important differences between the submitted version and the official published version of record. People interested in the research are advised to contact the author for the final version of the publication, or visit the DOI to the publisher's website.
- The final author version and the galley proof are versions of the publication after peer review.
- The final published version features the final layout of the paper including the volume, issue and page numbers.

[Link to publication](#)

General rights

Copyright and moral rights for the publications made accessible in the public portal are retained by the authors and/or other copyright owners and it is a condition of accessing publications that users recognise and abide by the legal requirements associated with these rights.

- Users may download and print one copy of any publication from the public portal for the purpose of private study or research.
- You may not further distribute the material or use it for any profit-making activity or commercial gain
- You may freely distribute the URL identifying the publication in the public portal.

If the publication is distributed under the terms of Article 25fa of the Dutch Copyright Act, indicated by the "Taverne" license above, please follow below link for the End User Agreement:

www.tue.nl/taverne

Take down policy

If you believe that this document breaches copyright please contact us at:

openaccess@tue.nl

providing details and we will investigate your claim.

Decay of dipolar vortex structures in a stratified fluid

J. B. Flór

Department of Applied Mathematics and Theoretical Physics, University of Cambridge, Silver Street, Cambridge CB3 9EW, England

G. J. F. van Heijst

J. M. Burgers Centre for Fluid Mechanics, Department of Technical Physics, Eindhoven University of Technology, P.O. Box 513, 5600MB Eindhoven, The Netherlands

R. Delfos

J. M. Burgers Centre for Fluid Mechanics, Laboratory for Aero and Hydrodynamics, Delft University of Technology, Rotterdamseweg 145, 2628AL Delft, The Netherlands

(Received 6 May 1994; accepted 5 October 1994)

In this paper the viscous decay of dipolar vortex structures in a linearly stratified fluid is investigated experimentally, and a comparison of the experimental results with simple theoretical models is made. The dipoles are generated by a pulsed horizontal injection of fluid. In a related experimental study by Flór and van Heijst [*J. Fluid Mech.* **279**, 101 (1994)], it was shown that, after the emergence of the pancake-shaped vortex structure, the flow is quasi-two-dimensional and decays due to the vertical diffusion of vorticity and entrainment of ambient irrotational fluid. This results in an expansion of the vortex structure. Two decay models with the horizontal flow based on the viscously decaying Lamb–Chaplygin dipole, are presented. In a first model, the thickness and radius of the dipole are assumed constant, and in a second model also the increasing thickness of the vortex structure is taken into account. The models are compared with experimental data obtained from flow visualizations and from digital analysis of particle-streak photographs. Although both models neglect entrainment and the decay is modeled by diffusion only, a reasonable agreement with the experiments is obtained. © 1995 American Institute of Physics.

I. INTRODUCTION

Since the advent of satellite imagery, coherent vortex structures have been found to be common features of many geophysical flows. Frequently dipolar vortex structures are observed at the ocean surface (Refs. 1 and 2), as well as in the atmosphere, better known as atmospheric blockings (Refs. 3 and 4). In these geophysical flows, the motion is, to first approximation, two dimensional due to background rotation and density stratification. In the laboratory, the emergence of dipolar structures, and their stability has been demonstrated in various kinds of experiments in two-dimensional flows, such as in a thin soap film,⁵ in magnetohydrodynamic flows,⁶ in rigidly rotating homogeneous flows,⁷ and in stratified rotating flows.⁸

The present study deals with the viscous decay of planar dipolar vortex structures in a nonrotating linearly stratified fluid. The dipolar vortex structures are generated by a short horizontal injection of fluid. By such an injection, an isolated turbulent region is formed that collapses under gravity. In the emerging quasi-two-dimensional flow eddies interact and merge, eventually leading to the dipole formation (Ref. 9). The formation process of dipoles in a stratified fluid, and their dynamics have been investigated in independent studies by the present authors (Refs. 10 and 11) and by Voropayev *et al.*¹² The latter authors, who considered, in particular, laminar injections of fluid, determined the horizontal entrainment rate experimentally, and by applying the principle of conservation of momentum they derived an expression for the dipole's decay for the inviscid case.

In their detailed study, Flór and van Heijst,¹⁰ henceforth

referred to as FvH, found that the theoretical Lamb–Chaplygin dipole model (Refs. 13–15) generally gives a good description of the midplane flow field of such dipoles in a stratified fluid. In that paper, also a scaling analysis of the vortical flow is presented, similar to that used by Riley *et al.*,¹⁶ from which it was found that the flow is quasi-two-dimensional and decays principally due to viscous diffusion in the vertical direction.

For the purely two-dimensional case, the viscous decay of the Lamb–Chaplygin vortex dipole has been investigated in an asymptotic expansion theory by Swaters,¹⁷ who showed that, under adiabatic constraints for the dipole radius and the linear streamfunction–vorticity relation, the dipole retains to leading order its basic properties and decays exponentially in time. Viscous effects on the stationarity of Lamb–Chaplygin dipoles have been investigated in an analytical-numerical study by Kida *et al.*,¹⁸ and it was shown that symmetry breaking may occur under certain conditions.

In a different approach, the decay of the final stage of turbulence in a stratified fluid was studied by Pearson and Linden,¹⁹ and by using linear theory they found an exponential decay of the most persistent wave numbers corresponding with horizontal quasi-two-dimensional motions.

In the present study, the viscous decay during the evolution of the flow process is investigated experimentally. In addition, two dipole decay models, both being based on a viscously decaying Lamb–Chaplygin vortex, as described by Swaters,¹⁷ are presented and compared with experimental results.

The paper is ordered as follows: The experimental setup, the visualization methods, and the method to obtain quanti-

tative information about the structure are presented in Sec. II. The observational analysis is discussed in Sec. III. After a short description of the principal equations of motion in a stratified fluid, a brief outline of the Lamb–Chaplygin model, and its viscous decaying variant are given, followed by a description of the decay models for a dipolar vortex. Subsequently, in Sec. V, the experimental results are compared with the models. A summary of the results is given in Sec. VI.

II. EXPERIMENTAL ARRANGEMENT

The majority of the experiments reported in this paper were performed in a Plexiglas tank of dimensions $30 \times 100 \times 100$ cm (height \times width \times length). The tank was filled with a linearly stratified salt solution, the stratification being established by the well-known two-tank method (see Ref. 20). The stratification was varied between $N=1.2$ and 3 rad/s, where N is the buoyancy frequency defined by $N = (-g/\bar{\rho} d\rho/dz)^{1/2}$ (with g the gravitational constant, $\bar{\rho}$ the mean density, and $d\rho/dz$ the density gradient with the vertical).

Dipolar vortices were created by a horizontal, pulsed injection of a small amount of fluid, which exactly matched the density of the ambient fluid at the plane of injection. The use of a computer-controlled injection mechanism allowed us to change the injection parameters (volume and speed). The Reynolds number of the injection $Re = Ud/\nu$, based on the injection velocity U , the nozzle diameter $d=2$ mm, and the kinematic viscosity ν , was varied between 360 and 11 500. As described in detail in FvH, the injected turbulent region quickly collapses under gravity, and a flat dipolar vortex structure emerges. The evolution of such flow structures was studied both by dye visualization and by streak photography of small tracer particles. The change in the dipole's translation velocity could be obtained from sequences of photographs taken at specific times.

In order to measure the evolution of the flow in a horizontal plane, small polystyrene particles of density 1.07 g/cm³ were added to the fluid and their motion was recorded by taking long exposure plan-view photographs. The tracer particles usually floated in a thin horizontal layer (typically 0.5 cm thick) at the level at which the injection also occurred. Before being injected, the injection fluid was siphoned from the layer containing the particles, to ensure that the injection fluid is of matching density. In this manner, the particles visualize the motion at the horizontal symmetry plane of the dipolar structure. Streak lengths were measured from an enlarged projection of the photograph by digitizing the ends of each streak. Dividing the path lengths by the exposure time yielded the local velocities. Subsequently, the velocity field was calculated on a rectangular grid of 30×30 grid points by numerical interpolation, using an algorithm described in some detail by NguyenDuc and Sommeria.⁶ From the thus obtained regular velocity field, the values of the vorticity ω and the streamfunction ψ of the planar flow field were calculated in each grid point. The mean extreme vorticity of the dipolar flow field was defined by $\omega_m = \frac{1}{2}(\omega_{\max} - \omega_{\min})$, while the mean circulation Γ was calculated by taking the summation of the vorticity values $\omega_{i,j}$

over all the grid points (i,j) according to $\Gamma = \frac{1}{2} \sum_{i,j} |\omega_{i,j}| \Delta x \Delta y$, where $\Delta x \Delta y$ is the surface of one mesh of the grid. For the calculation of the circulation Γ , a threshold value of $0.05 \omega_m$ was built in to filter the noise in the vorticity near $\omega=0$.

Information about the vertical distribution of the horizontal velocity and about the vertical growth of the dipole region was obtained in additional experiments carried out in a smaller tank (of dimensions $35 \times 50 \times 80$ cm, height \times width \times length), by creating a vertical dye line in the middle of the tank after the dipole was formed. The dye lines were created with a thin solder wire of diameter 0.5 mm by the precipitation method (see Ref. 21), and could be produced at any desirable moment. Having a light grey color, their displacement due to the translating dipolar structure was clearly visible against a black background, and was recorded from the side by a photcamera. Although in a number of experiments asymmetric dipoles were formed (in such cases some amount of vorticity was partly left behind in the wake of the dipole), care was taken that in all cases discussed in the present paper the dipoles were symmetric and exactly aligned with the vertical electrode wire. Some of the recorded dye-lines distortions were digitized by hand in order to obtain quantitative information about the vertical distribution of the horizontal velocity field. In a number of experiments, dye was also added to the injected fluid, so that the dipolar vortex region and the displacement profile were visible simultaneously. Then, the dipole thickness was measured from the displacement profile at the position exactly between the vortex centers.

III. QUALITATIVE OBSERVATIONS AND ANALYSIS

After the pulsed injection, an isolated turbulent region forms, which collapses under gravity to a thin pancake-shaped region, after which a quasi-two-dimensional flow is established. In this quasi-two-dimensional flow, horizontal eddies interact and merge, a process that leads to the eventual formation of a dipolar structure (see Ref. 11 and FvH). Internal waves, generated by the initial pulsed injection and the subsequent gravitational collapse of the turbulent patch, are observed to vanish quickly, in particular after having been reflected at the tank walls. Once the dipolar vortex has been formed, these internal waves have a very small amplitude and appear to have a negligible effect on the dipolar vortex structure, which translates quasisteadily along a straight trajectory.

Figure 1 shows a combined top and side view of the eventual dipolar vortex structure, visualized by fluorescein dye. A mirror was placed under an angle of 45° along the sidewall of the tank, so that plan view and side view could be recorded simultaneously by a single camera. The photograph in Fig. 1 clearly reveals the pancake-like shape of the visualized vortex region: the horizontal scale is much larger than the vertical length scale. In view of this shape one may define two different Reynolds numbers: a horizontal Reynolds number $Re_h = U_0 D/\nu$, based on the translation velocity U_0 of the dipole and its diameter D , and a vertical Reynolds number $Re_v = 2\sigma U_0/\nu$, with 2σ a measure for the dipole thickness. Soon after the dipole formation is completed, the

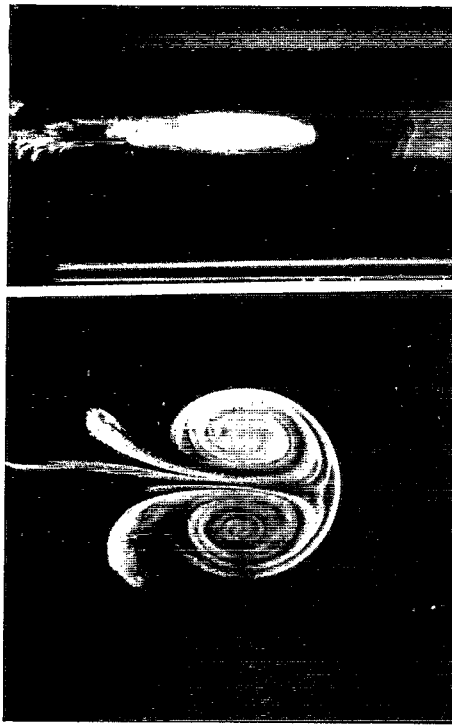


FIG. 1. Photograph showing the top view and side view (lower and upper part of the picture, respectively) of the dye-visualized dipolar flow. Experimental parameters: $Q=2$ ml/s, $\delta t=1.5$ s, and $N=1.7$ rad/s.

Reynolds numbers have typical values $Re_h=1000$ and $Re_v=300$. During the course of an experiment, these values decrease rapidly to lower values of $O(100)$ and $O(10)$, respectively, indicating that viscous effects associated with vertical diffusion of vorticity are most significant. Due to this vertical diffusion and the horizontal entrainment of ambient irrotational fluid, the structure grows in size, which leads to a gradually decreasing translation velocity.

Plan-view dye visualizations reveal spiraled-shaped dye patterns due to the entrainment of ambient uncolored fluid. Since vorticity filaments have large vorticity gradients and consequently diffuse, a continuous vorticity distribution forms rapidly. Because of the high Schmidt number, the dye displays a different behavior, and represents more the history of the flow. However, it is assumed that at the dipole's edge, where vorticity gradients are relatively small, the dye region represents in good approximation the horizontal size of the structure.

In order to examine the vertical growth of the dipole and the vertical distribution of the horizontal motion due to the moving dipole, a vertical dye line was generated on the horizontal symmetry axis of the structure. While the vertical size of the dipole increases by diffusion of vorticity, the dye line is horizontally advected over an increasing vertical distance. In this way information is obtained about the dipole's vertical expansion. As shown in Figs. 2(a)–2(c), the vertical scale of this displacement profile increases by almost a factor of 2 during the period from $t=47$ s to $t=107$ s. In separate experiments, the horizontal size D of the dye distribution (defined as the maximum dipole width perpendicular to the

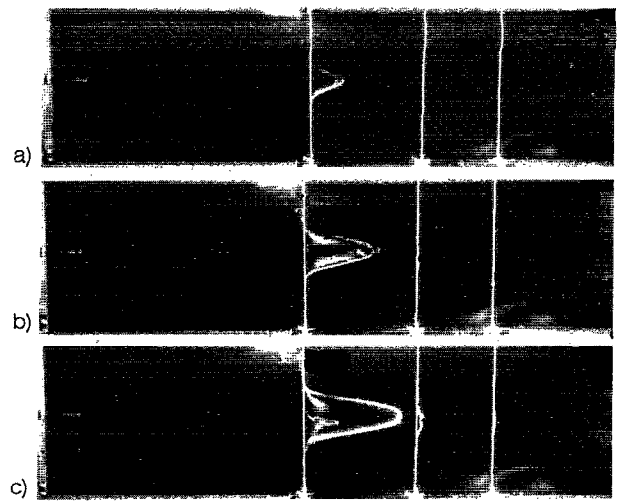


FIG. 2. Sequence of photographs showing the deformation of a vertical dye line due to a horizontally moving dipole with a radius of approximately 10 cm; the photographs are taken at (a) $t=47$ s, (b) $t=61$ s, and (c) at $t=107$ s, after injection at $t=0$ s. The dye line is created with the precipitation method. Experimental parameters: $Q=2.5$ ml/s, $\delta t=0.6$ s, $N=1.5$ rad/s, and nozzle diameter $d=1.1$ mm. The top–bottom distance in each picture represents the scale, and is 18.3 cm.

translation direction) was measured from dye visualizations. Typical graphs of the measured expansion of the vortex region in horizontal and vertical direction are shown in Figs. 3(a) and 3(b), respectively. Apparently, the rate of vertical expansion by diffusion is much larger than the horizontal expansion rate, which is mainly an effect of entrainment. Therefore, one may expect that, apart from the effect of entrainment, vertical diffusion of vorticity determines the decay of this pancake-like vortex structure.

According to the side view part of Fig. 1, the dyed fluid is confined in a thin layer, suggesting a considerable shear at the top and bottom edges of the structure. However, the dye-lines of Figs. 2(a)–2(c) reveal a very smooth Gaussian-like profile, indicating that overturning motions by the shear as well as vertical motions by internal waves are insignificant. For this flow, one can define the bulk Richardson number, which is the ratio of the restoring buoyancy forces and the inertial forces, as $Ri=N^2/(\partial U/\partial z)^2$. With typically $N=1.5$ rad/s, $U_0=0.5$ cm/s and a typical thickness $2\sigma\approx 5$ cm, this number is $Ri\sim O(100)$, indicating a buoyancy-dominated flow. With a decreasing velocity U_0 and an increasing layer thickness 2σ , the Ri number rapidly increases in time, so that no overturning motions are to be expected in the further dipole evolution. The deformations of the dye line in the two subsequent pictures [Figs. 2(b) and 2(c)] are digitized by hand, and both are fitted (by eye) with a Gaussian curve of the form $\exp(-z^2/2\sigma^2)$, where z is the vertical coordinate with $z=0$ at the midplane, and σ is a measure for the dipole thickness, respectively. The results are shown in Fig. 4. The displacement profiles appear to be self-similar in time. By subtracting two digitized profiles, a similar Gaussian-like distribution for the horizontal velocity was found.

It was argued in FvH that vortex lines are locally perpendicular to the midplane $z=0$; at higher levels the vortex

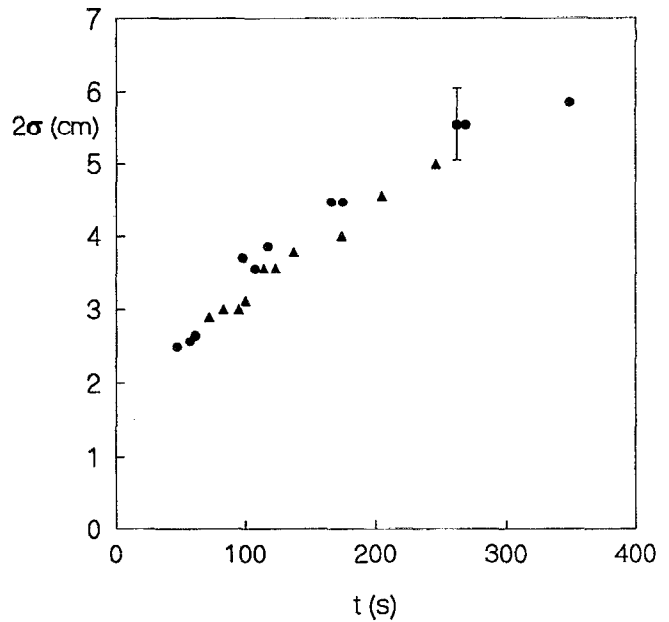
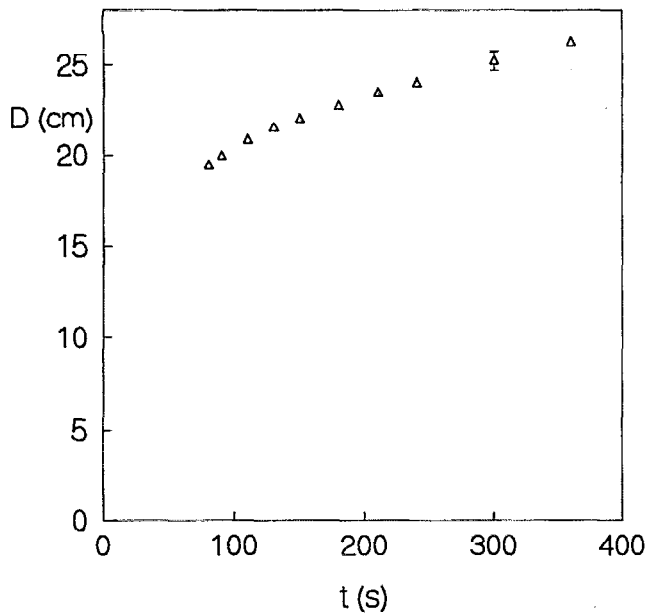


FIG. 3. Graphs showing typical evolutions of (a) the dipole diameter D and (b) the dipole thickness 2σ . Experimental parameters: (a) see Table I, experiment 07; (b) ●, $Q=2.0$ ml/s, $\delta t=0.3$ s, $N=1.8$ rad/s, and $d=1.1$ mm; ▲, $Q=4.1$ ml/s, $\delta t=0.3$ s, $N=2.0$ rad/s, and $d=2.0$ mm.

lines are tilted by the shear, but the motion remains planar and vertical motions are negligible.

IV. MODELS OF DECAYING DIPOLAR VORTICES

As a first approximation in the modeling of the decay of a planar dipolar vortex, it is assumed that the motion is confined mainly in a thin (disk-shaped) region around the mid-plane, where the vorticity vectors are directed vertically, and the vortex tilting by the shear is negligible. Since the mid-

plane is a maximum of a smooth Gaussian-like velocity profile with growing thickness, this is a reasonable approximation for the flow in a thin layer around $z=0$.

For the dipolar vortex, the horizontal flow at the mid-plane is described quite well by the Lamb–Chaplygin dipole model (see FvH), so that for the present decaying flow the viscous decaying Lamb–Chaplygin dipole, as described by Swaters,¹⁷ can be used. The dipole radius is assumed constant, neglecting the effects of entrainment and implying a purely viscous decay. In view of the displacement profiles observed in the experiments, the vertical distribution of the horizontal velocity is taken to be Gaussian. The dipole's translation velocity at the midplane is a measure for the amplitude of the translation velocity of the dipole, and according to the Lamb–Chaplygin dipole model also for the amplitude of characteristic properties such as the vorticity and the circulation for each dipole half. As a first step a model dipole with a constant thickness is presented. Next, a more refined model is presented, which allows for a growing dipole thickness due to the vertical diffusion of vorticity.

A. Viscous decay in buoyancy-dominated flows

By using a scaling analysis, similar to that given by Ref. 16, it was shown in FvH that the vertical vorticity of buoyancy dominated flows is to first order governed by

$$\frac{\partial \omega_z}{\partial t} + J(\omega_z, \psi) = \frac{1}{\text{Re}_h} \nabla_h^2 \omega_z + \frac{1}{\alpha \text{Re}_v} \frac{\partial^2 \omega_z}{\partial z^2}, \quad (1)$$

with the streamfunction ψ defined by $\mathbf{u}_h = -\mathbf{k} \times \nabla \psi$, $\nabla^2 \psi = -\omega_z$ and J the Jacobian defined by $J(\omega, \psi) = (\partial \omega / \partial x)(\partial \psi / \partial y) - (\partial \omega / \partial y)(\partial \psi / \partial x)$. The constant α is the aspect ratio between horizontal and vertical length scales and is here of the order $O(0.1)$. For the present observations the horizontal Reynolds number Re_h is much larger than the ver-

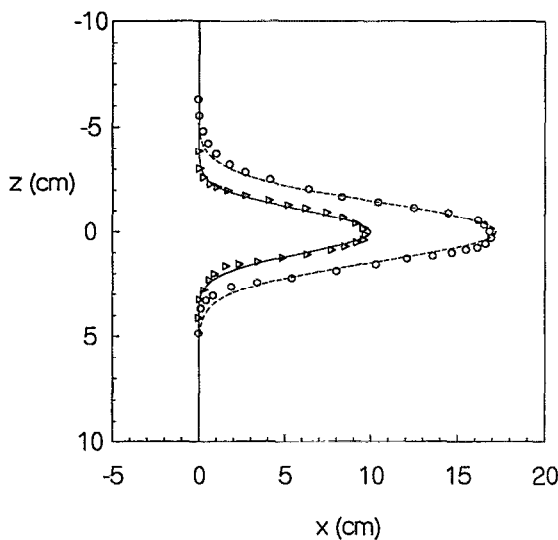


FIG. 4. Typical vertical displacement profiles digitized from pictures, as shown in Fig. 2, at $t=40$ s, and $t=80$ s after injection at $t=0$ s, denoted by the symbols ▽ and ○, respectively. Both profiles are fitted by hand with a Gaussian curve of the form $U=U_0 \exp(-z^2/2\sigma^2)$, with 2σ the typical thickness of the dipole.

tical Reynolds number Re_v ($Re_v = \alpha Re_h$), indicating that the viscous decay is mainly due to vertical diffusion. The inviscid part of Eq. (1) is identical to the vorticity equation of purely two-dimensional flow. On the short advective time scales, one can define stationary (inviscid) solutions by a relation $\omega = F(\psi)$, with F an integrable function. Assuming that such a relationship exists, the nonlinear term in the vorticity equation vanishes, and (1) reduces to leading order to

$$\frac{\partial \omega_z}{\partial t} = \frac{1}{\alpha Re_v} \frac{\partial^2 \omega_z}{\partial z^2}, \quad (2)$$

which describes diffusive decay. Because horizontal vortex motions are to lowest-order decoupled from vertical motions and internal waves—with consequently their radiation of energy—the vertical vorticity ω_z decays mainly due to this vertical diffusion. Although in the present stratified flow the vertical diffusion term is much larger than the horizontal diffusion term, both will be kept in the further analysis; on very large time scales the ratio $\alpha Re_v / Re_h = (\sigma/D)^2$ increases, so that then the horizontal diffusion term might become significant. The vorticity equation then yields (in dimensional units)

$$\frac{\partial \omega}{\partial t} + J(\omega, \psi) = \nu \nabla_h^2 \omega + \nu \frac{\partial^2 \omega}{\partial z^2}, \quad (3)$$

where the indices z have been dropped.

B. The viscously decaying Lamb–Chaplygin dipole

The Lamb–Chaplygin dipole model (Refs. 13 and 14) assumes a linear relation $\omega = k^2 \psi$ (with k a constant) within an isolated circular region with radius $r = a$, and a potential flow $\omega = 0$ in the exterior region ($r > a$). The solution in terms of the streamfunction of the flow, relative to a comoving frame with velocity U_0 , is

$$\begin{aligned} \psi &= -\frac{2U_0}{kJ_0(ka)} J_1(kr) \sin \theta, \quad \text{for } r \leq a, \\ \psi &= U_0 \left(r - \frac{a^2}{r} \right) \sin \theta, \quad \text{for } r \geq a, \end{aligned} \quad (4)$$

where J_1 is the first-order Bessel function of the first kind. Continuity of the velocity at $r = a$ requires

$$ka = 3.8317, \quad (5)$$

which represents the first zero of J_1 . According to this model, the dipole is characterized by two quantities: its radius—or alternatively by k according to relation (5)—and its translation velocity U_0 . A few characteristics, to be referred to later in this paper, are the magnitude of the maximum vorticity ω_m , the maximum velocity U_{\max} relative to a comoving frame of reference, and the circulation Γ contained in each dipole half. These values can be expressed in terms of U_0 and k :

$$\begin{aligned} \omega_m &= 2.89kU_0, \\ U_{\max} &= 2.49U_0, \\ \Gamma &= 26.17U_0/k. \end{aligned} \quad (6)$$

The viscous decay of a purely two-dimensional vortex is governed by (3), with the last term being zero. In the particular case of a linear relationship $\omega = k^2 \psi$, one obtains an exponential decay,

$$\omega = \omega_0(x, y) \exp(-t/\tau_{2d}), \quad (7)$$

with $\omega_0(x, y)$ the vorticity according to the Lamb–Chaplygin solution, and the decay time defined as (see Refs. 14 and 15)

$$\tau_{2d} = (\nu k^2)^{-1}. \quad (8)$$

In a perturbation approach (valid for small time scales), Swaters¹⁷ studied the two-dimensional effects of viscosity, and, under the constraints that to leading order the dispersion relationship (5) and the relation $\omega = k^2 \psi$ are maintained, he found that the radius of the Lamb–Chaplygin dipole kept its initial value. The diffusion of the kink in the vorticity on the circle $r = a$ only leads to small effects, as was shown by Kida *et al.*¹⁸ The latter authors estimated this deviation from the Lamb–Chaplygin dipole in terms of the dipole radius and circulation Γ , and showed that on a time scale $t \sim a^2/\Gamma$ [$\sim O(1 \text{ s})$], a front–back asymmetry occurs in a thin band with thickness $\approx O(a\sqrt{\nu/\Gamma})$ ($\sim 0.1 \text{ cm}$) at this circular boundary, while for $t_v \approx a^2/\nu$, the viscous layer spreads out over the whole structure. However, as long as $t \ll t_v$, this effect is negligible, so that the dipole may be considered as a stationary structure for which the Jacobian is approximately zero. In this paper, the smallest dipole had a radius $a \approx 5 \text{ cm}$, implying $t_v = 2500 \text{ s}$, while for all experiments $t < 400 \text{ s}$, so that this condition is satisfied.

C. The constant-thickness model

Although the viscous Lamb–Chaplygin model describes a two-dimensional flow, with vorticity diffusing in the horizontal plane, the experimental observations reveal a flat dipolar vortex structure with an increasing thickness, and vertical vorticity diffusing in vertical direction. As a first step in the description of this vortex structure the flow is modeled by a Lamb–Chaplygin dipole with a constant thickness σ , and some prescribed vertical variation in its “amplitude” U_0 . This model is referred to as the “constant thickness model.” As shown in Fig. 4, the vertical displacement profile of the dipole can be approximated quite well by a Gaussian fit, and the vertical distribution of the horizontal velocity is described by a similar profile, i.e., $U_0 \sim \exp(-z^2/2\sigma^2)$. The vertical scale σ of this profile is assumed constant in time. Because of the symmetry of the dipolar structure about the midplane the characteristic dipole thickness is then 2σ . For the present buoyancy-dominated flow, where vertical motions are to leading order decoupled from the horizontal motions, we assume that in each horizontal plane the motion is that of a decaying Lamb–Chaplygin dipole, with a translation velocity of amplitude $\sim U_0 \exp(-z^2/2\sigma^2)$. This assumption is valid in the region $z/\sigma \ll 1$, where (since $\partial u_h/\partial z \approx 0$) the vorticity vector is directed approximately vertically. The vorticity distribution is then

$$\omega(x, y, z, t) = \omega_0(x, y) \exp(-z^2/2\sigma^2) h(t), \quad (9)$$

where $\omega_0(x, y)$ represents the horizontal distribution of the vertical vorticity component according to the Lamb–

Chaplygin solution, and $h(t)$ is a time-dependent amplitude function. When (9) is substituted in Eq. (3), the Jacobian term is found to vanish, implying a diffusive decay according to

$$\frac{\partial \omega}{\partial t} = \nu \left(-k^2 - \frac{1}{\sigma^2} + \frac{\epsilon^2}{\sigma^2} \right) \omega, \quad (10)$$

where $\epsilon = z/\sigma$. For $\epsilon \ll 1$, or more precisely $\epsilon \ll (1 + \sigma^2 k^2)^{1/2}$, one obtains

$$\omega(x, y, z, t) = \omega_0(x, y) \exp\left(\frac{-z^2}{2\sigma^2}\right) \exp\left(\frac{-t}{\tau_{ct}}\right) - O\left(\frac{\nu \epsilon^2 t}{\sigma^2}\right), \quad (11)$$

with

$$\tau_{ct} = (\nu \lambda^2)^{-1}, \quad (12)$$

the decay time, and $\lambda^2 = k^2 + 1/\sigma^2$. For $t \ll \sigma^2/\nu \epsilon^2$, the last term in (11) can be neglected. In the experiments $t < 400$ s, implying that for a minimal thickness $\sigma = 1$ cm, Eq. (11) may be used in the region where $|z| \leq \sigma/2$. The vorticity amplitude decays exponentially with a decay time (12), which is, for the present experiments, primarily determined by the thickness of the dipolar structure. The decay time τ_{ct} is short compared to the time scale τ_{2d} given by (8).

D. Vertical diffusion model

A more accurate model is obtained when the vertical diffusion of (vertical) vorticity is allowed to result in a vertical growth of the dipolar structure like observed in the experiments (see Fig. 2). For this diffusion model it is only assumed that the horizontal planar flow is represented by the Lamb–Chaplygin dipole model. As above, the model will be only valid in a thin region around the midplane level, where $\partial \mathbf{u}_h / \partial z \approx 0$. This yields

$$\omega = \omega_0(x, y) \gamma(z, t), \quad (13)$$

where $\omega_0(x, y)$ is again the horizontal vorticity distribution according to the Lamb–Chaplygin dipole, and $\gamma(z, t)$ is an amplitude function. Substitution of (13) in (3) yields

$$\frac{\partial \gamma}{\partial t} = -\nu k^2 \gamma + \nu \frac{\partial^2 \gamma}{\partial z^2}. \quad (14)$$

By the transformation $\gamma = \Phi(z, t) \exp(-\nu k^2 t)$ one obtains a diffusion equation for $\Phi(z, t)$:

$$\frac{\partial \Phi}{\partial t} = \nu \frac{\partial^2 \Phi}{\partial z^2}. \quad (15)$$

It is assumed that initially the vorticity is confined to a thin region, according to $\Phi(t=0) = \Phi_0 \delta(z)$, with δ the Dirac delta function. The associated source solution is then given by

$$\Phi = \frac{1}{\sqrt{4\nu t}} \exp\left(\frac{-z^2}{4\nu t}\right). \quad (16)$$

Although the flow at $t=0$ is still three-dimensional turbulent and the actual ω distribution is strictly not described by this particular delta-like initial condition, one may assume that

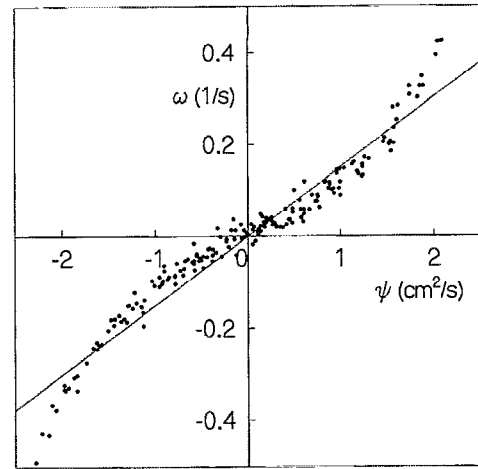


FIG. 5. Typical nonlinear ω, ψ scatter plot measured for a dipolar structure, fitted with a least-square linear fit in order to determine the value k^2 .

the details of the initial vorticity distribution are lost at larger t values when the dipolar structure has been formed and that (16) then still gives a reasonable description.

The solution for the vorticity $\omega(x, y, z, t)$ thus found is

$$\omega = \omega_0(x, y) \frac{1}{\sqrt{t}} \exp\left(\frac{-t}{\tau_{dif}}\right) \exp\left(\frac{-z^2}{4\nu t}\right), \quad (17)$$

where

$$\tau_{dif} = (\nu k^2)^{-1}. \quad (18)$$

This time scale is identical to the value τ_{2d} ; see (8). Integration of (17) in the z direction yields again the expression for diffusion in a two-dimensional flow, given by Eq. (7). As in other diffusion problems, the thickness of the diffusing region grows according to $\sigma(t) \sim \sqrt{\nu t}$. The factor $4\nu t$ in (17) is directly associated with the factor $2\sigma^2$ of the Gaussian profile as described by (9) and represents the vertical growth of the vortical region. It should be noted that with Eq. (6a) a similar expression for the decay of the velocity U_0 can be obtained.

V. COMPARISON WITH THE EXPERIMENTAL RESULTS

In order to compare the two models with the experimental decay values, the decay times for the maximum vorticity and the circulation are measured from the interpolated velocity field.

The translation velocity U_0 of the dipole was determined directly from streakline pictures by measuring the longest particle path on the symmetry axis, since, according to the Lamb–Chaplygin model, $U_{\max} = 3.49 U_0$. In the experiments reported by FvH, it was shown that this provides a good approximation of the translation velocity. By processing a sequence of streak pictures the decay of ω_m , Γ , and U_0 could be displayed as a function of time, and the experimental decay times τ_{ct} and τ_{dif} for the parameters velocity U_0 , circulation Γ , and maximum vorticity ω_m could be determined. Separately, the wave number k was measured from ω, ψ scat-

TABLE I. The experimental parameters (columns 2–4) and the exponential decay times obtained from these experiments, calculated according to the constant-thickness model. The decay of the velocity U_0 , maximum vorticity ω_m , and circulation Γ are presented in a log-linear plot in Figs. 7(a)–7(c), respectively. The decay time $(\nu\lambda^2)^{-1}=(\nu k^2+\nu/\sigma^2)^{-1}$ is obtained from the radius of the dipole, or scatter plots as shown in Fig. 5, and the thickness σ (see the text). In addition, the decay values ω_m/a and Γ/a , which are corrected for the radial growth, are presented. The experiments where the decay in circulation and vorticity are given, concern those experiments where information is obtained from streak pictures, while the other four experiments concern the color visualizations.

Exp. No.	Q ml/s	δt s	N rad/s	$\tau_{ct}(U_0)$ s	$\tau_{ct}(\Gamma)$ s	$\tau_{ct}(\Gamma/a)$ s	$\tau_{ct}(\omega_m)$ s	$\tau_{ct}(\omega_m a)$ s	$(\nu\lambda^2)^{-1}$ s
01	0.6	25.0	3.0	80± 6	88± 6	78± 8	80± 4	91± 4	74± 18
02	11.2	0.7	2.2	177±25	189±25	148±43	139±30	208±40	297±88
03	11.2	0.3	2.2	181±13	208±13	161± 8	112± 6	130±10	255±73
04	8.7	0.26	2.3	175± 9	196±15	169±20	117± 8	133±11	246±78
05	16.8	0.2	2.1	171±12	221±24	172± 9	118± 4	137± 6	278±71
06	9.2	0.4	1.7	196±15					237±68
07	6.1	0.6	1.7	172±12					232±63
08	9.2	0.4	1.4	176± 6					232±70
09	12.2	0.2	1.2	225±25					306±82

ter plots, such as shown in Fig. 5 (note that according to the Lamb–Chaplygin dipole, the slope of the linear ω, ψ relationship is, by definition, equal to k^2), which yields the value of the decay time τ_{2d} . Although both linear and nonlinear ω, ψ relations have been found (see FvH), a least-square linear fit was used to obtain the value of k^2 . The value k^2 obtained by this method was found to agree quite well with that predicted by the Lamb–Chaplygin model, for the linear as well as for the nonlinear ω, ψ dipoles. Because the radius of the dipole slightly increases during the decay process—and therewith k^2 decreases—the average of k^2 values of one sequence of streak pictures is used to calculate a mean value of τ_{2d} for the experiment, while the variation in k^2 determines the standard deviation in τ_{2d} .

In additional dye-visualization experiments, the velocity of the dipole was measured from the displacement of the dye pattern, and the decay time scales τ_{ct} and τ_{dif} were determined from the decay of this translation velocity. Then, the corresponding wave number k was derived from the mean radius of the dipole by using relation (5), yielding the value of τ_{2d} , while the standard deviation of τ_{2d} is again given by the variation in this radius. The experimental parameters of the experiments that have been analyzed are presented in Table I, with the derived decay times according to the constant-thickness model; the decay times according to the vertical diffusion model are presented in Table II.

A. Comparison with the constant thickness model

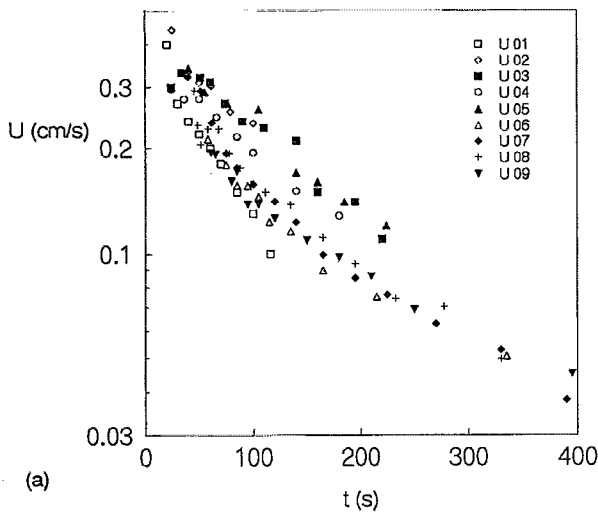
Figures 6(a)–6(c) show the behavior of the measured quantities U_0 , ω_m , and Γ (at $z=0$), respectively, as a function of time, within each graph the ordinate axis taken logarithmic, so that an exponential decay is displayed by a straight line. Apparently all quantities appear to have an approximately exponential decay. The data of each experimental run were least-square fitted with an exponential curve and provided a value for τ_{ct} . Independently, the value $\nu\lambda^2=\nu k^2+\nu/\sigma^2$ was determined. As mentioned, an average k^2 value was obtained from the scatter plots. From the laboratory observations (experiments 06, 07, and 08), the thickness 2σ was estimated roughly by eye as 4 ± 1 cm for most of the experiments. Experiment 01 concerned a laminar injection of fluid, so that a very thin vortex region was formed with a thickness typically of $2\sigma=2\pm 1$ cm; in experiment 09 a weak stratification was used in combination with a very intense turbulent injection, resulting in a dipolar structure with a relatively large thickness of typically 5 ± 1 cm. The measured decay times $\tau_{ct}(U_0)$ are of the same order as the “theoretical” decay time $(\nu\lambda^2)^{-1}$. The deviations are due to the rough estimation of the thickness σ and the error in the k^2 value, which was determined by averaging k^2 in time.

Although the values for the decay time of the maximum vorticity ω_m vary from those of the velocity U_0 (see Table I), they show a similar trend. From the expressions for ω and Γ as given by (6), it is obvious that a growth in radius $a\sim 1/k$ induces a slow decay in Γ and a fast decay in ω_m . In order to obtain comparable decay times as for the velocity U_0 , the decay of $\omega_m a$ and Γ/a are calculated and listed in Table I as $\tau_{ct}(\omega_m a)$ and $\tau_{ct}(\Gamma/a)$, where a is now the time-dependent radius. The decay time $\tau_{ct}(\Gamma/a)$ is generally in better agreement with the decay time obtained for the translation velocity. However, the decay time $\tau_{ct}(\omega_m a)$ is, on average, still smaller than $\tau_{ct}(U_0)$ and $\tau_{ct}(\Gamma/a)$, thus implying a faster decay of vorticity in the vortex centers than elsewhere in the dipole. An explanation for this effect lies in the fact that the

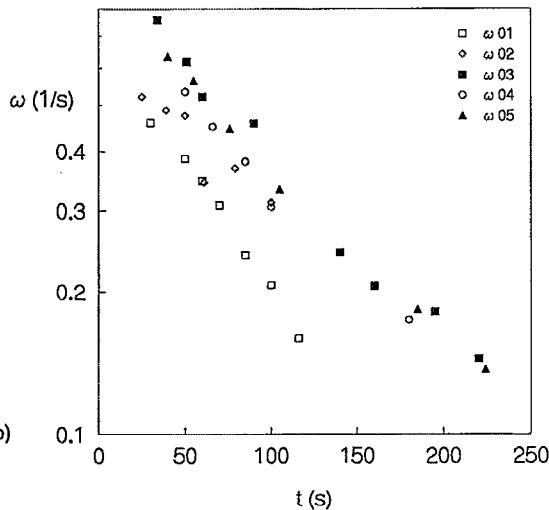
tion of fluid, so that a very thin vortex region was formed with a thickness typically of $2\sigma=2\pm 1$ cm; in experiment 09 a weak stratification was used in combination with a very intense turbulent injection, resulting in a dipolar structure with a relatively large thickness of typically 5 ± 1 cm. The measured decay times $\tau_{ct}(U_0)$ are of the same order as the “theoretical” decay time $(\nu\lambda^2)^{-1}$. The deviations are due to the rough estimation of the thickness σ and the error in the k^2 value, which was determined by averaging k^2 in time.

TABLE II. As in Table I, but now the decay times τ_{dif} according to the diffusive damping model, where $U\sim 1/\sqrt{\nu t}\exp(-t/\tau_{dif})$, are compared with the decay times τ_{2d} . These decay times are obtained from fits as shown in Figs. 8(a) and 8(b), with the curve $1/\sqrt{\nu t}\exp(-t/\tau_{dif})$. Because for these approximations long runs were needed, some of the experimental runs presented in Table I are omitted here.

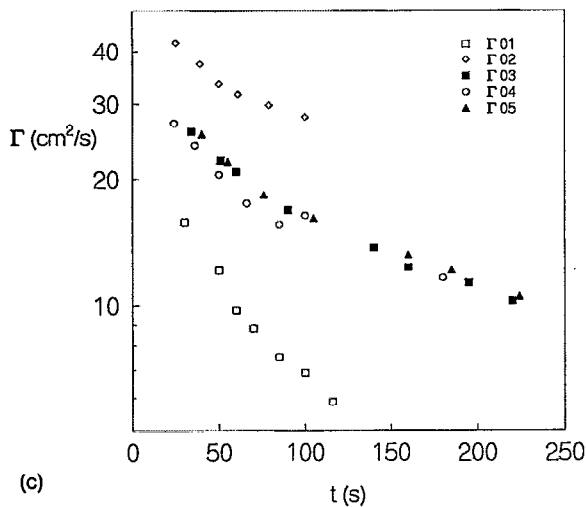
Exp. No.	$\tau_{dif}(U)$ s	$\tau_{dif}(\omega_m)$ s	$\tau_{dif}(\omega_m a)$ s	$(\nu k^2)^{-1}$ s
01	312± 30	141±14	294±40	288± 22
03	540±154	243±24	345±36	676± 114
04	666± 44	263±21	345±59	643±123
05	1111±247	256±13	352±25	911± 46
06	483± 47			583± 79
07	417± 17			550± 60
08	454± 41			552± 92
09	559± 47			600± 60



(a)



(b)



(c)

FIG. 6. Graphical display of the temporal evolution of (a) the translation velocity, (b) the maximum vorticity ω_m , and (c) the mean circulation Γ of the dipole. The experimental parameters are presented in Table I.

observed dipoles in the experiments generally have a nonlinear ω, ψ relation, while a linear relation is assumed. Nonlinear dipoles have a higher vorticity in the vortex centers, with sharper gradients in the vorticity than expected according to

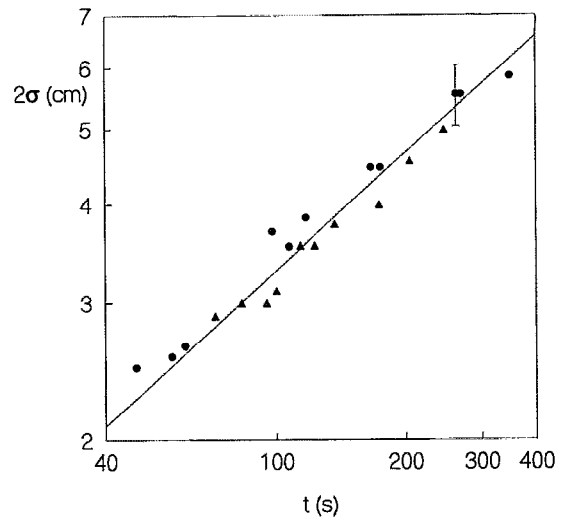


FIG. 7. Graph showing the data of Fig. 3(b), fitted by the curve $2\sigma = 4\sqrt{vt/\beta}$, according to the vertical diffusion model.

the linear ω, ψ relation. Then, the spreading of vorticity over a larger area has a larger effect on the maximum vorticity than on the total circulation. For comparison, a dipole with a linear ω, ψ relation, such as in experiment 06, shows approximately the same decay times for ω_m and U_0 .

In conclusion, the experimental results show that the decay of the translation velocity of the dipole is in reasonable agreement with the constant thickness model. Differences in decay with the measurements become of importance only on large time scales, for which the approximation of a constant thickness is not valid anymore.

B. Comparison with the vertical diffusion model

Figure 7 shows the typical growth in total thickness (2σ) of the dipolar structure plotted in a logarithmic graph, compared with a least-square fit of the curve $2\sigma = 4\sqrt{vt/\beta}$, where β is a free parameter. According to the diffusion model (17), the parameter $\beta=1$, while for the constant thickness model this parameter was taken equal to 2 [see the z -dependent factor exponential factor in (11)]. However, the fit made in Fig. 7 yields the β value $\beta=1.47\pm 0.04$, which implies that the dipole thickness grows slower than according to the diffusion model. This is due to the shear not being incorporated in this model. Apparently, the thickness corresponds with the region where the velocity amplitude exceeds the value $\exp(-1/\beta)U_0 \approx \exp(-\frac{2}{3})U_0 \approx 0.5U_0$, with U_0 the maximum velocity at $z=0$. This layer thickness is slightly larger than the thickness determined by the levels with maximum shear, i.e., at $z=\sigma$, with $\exp(-\frac{1}{2})U_0 \approx 0.6U_0$, which suggests that the dipole thickness is defined by these levels.

Figures 8(a) and 8(b) present the temporal evolution of the translation velocity $U_0(t)$ and the maximum vorticity $\omega_m(t)$, respectively, for three different experiments, with a comparable decay time τ_{2d} . In both graphs the data of one of the experiments are fitted by Eq. (17) of the vertical diffusion model (for $z=0$), and both show a very good agreement.

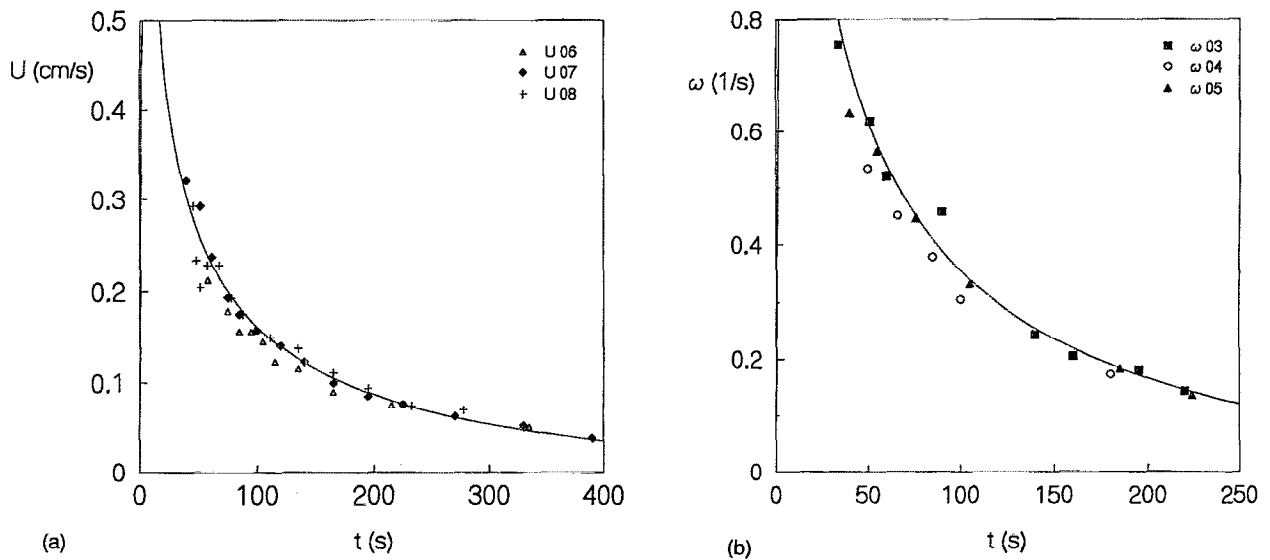


FIG. 8. Graphs showing the measured evolution of the dipole translation velocity U for the three different experiments (06, 07, and 08) in which the dipole had approximately the same radius, and (b) the measured evolution of the extreme vorticity ω_m for the experiments 02, 04, and 05 (values of the experimental parameters are given in Table I). The curves represent Eq. (17) and have been least-square fitted to experiment 07 (a) and 03 (b).

The decay values $\tau_{\text{dif}}(\omega_m)$ and $\tau_{\text{dif}}(U_0)$ obtained from fits as shown in Figs. 8(a) and 8(b) are listed in Table II. The decay times $\tau_{\text{dif}}(U_0)$ are, generally, in very good agreement with the decay times $\tau_{2d}(k^2)$ obtained by measuring the radius of the dipole. Also in this model, it appears that ω_m decays faster than the translation velocity U_0 , while a correction for the increasing radius yields similar results as for the constant-thickness model.

The data for the circulation Γ contained too much scatter to make a proper fit, and was therefore not used for further calculations. This scatter is probably due to small three-dimensional effects. In conclusion, the diffusion model describes the decay of the dipolar vortex quite well. The effect of the vertical growth of the dipole is included, and the validity of the model holds for a much longer time. In view of the large data runs needed for a reasonable fit for the diffusion model, on short time scales the constant thickness gives a useful approximation.

VI. CONCLUSIONS AND DISCUSSION

The aim of this study was to investigate the decay of planar dipolar vortex structures in a stratified fluid. Qualitative and quantitative information was obtained from flow visualization techniques, as well as from particle-streak photography. The observed dipolar structure can be characterized as a laminar coherent vortex motion, confined in a thin layer of fluid. By diffusion of vorticity, the volume of the structure grows both vertically and horizontally, whereby its horizontal velocity field is characterized by an approximately Gaussian distribution $\sim \exp(-z^2/2\sigma^2)$ in the vertical direction. The dipole thickness is defined by the levels of maximum shear.

For the near-midplane horizontal flow region, where the shear is negligible, two decay models have been formulated, based on the viscously decaying Lamb–Chaplygin dipole (Swaters¹⁷). A constant-thickness model is developed, with

the diffusion of momentum in vertical and horizontal directions. The predicted decay and thickness values are in reasonable agreement with the experimental data, although for large times the neglected vertical growth becomes of importance, and the validity of the model becomes doubtful.

The diffusion model, according to which vertical diffusion of vorticity induces an increasing thickness, shows a very good agreement also for large times. The vertical expansion of the dipole shows the same tendency as predicted by the model, and is $\sim \sqrt{\nu t}$. The difference in the theoretical proportionality constant and that measured in the experiments is due to the neglected effects of horizontal advection of vorticity, which cause a slower growth.

In Fig. 9 the decay in vorticity for both models is plotted

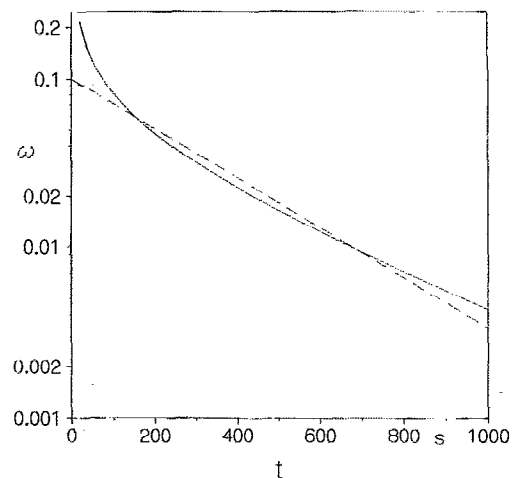


FIG. 9. Graphical representation of the decay in vorticity according to relation (11) and relation (17) of the constant-thickness model (dashed line) and the diffusion model (drawn line), respectively. The amplitudes in both relations are matched by hand for $t \approx 150$ s.

as a function of time for the case $\tau_{2d} = 1/(\nu k^2) = 500$ s. From the relation $\sigma = \sqrt{2\nu t}$, an average value of σ^2 was determined for the range $0 \leq t \leq 400$ s, thus providing a value for $\tau_{ct} = (\nu k^2 + \nu/\sigma^2)^{-1}$. Figure 9 shows that, in the range between $t \approx 100$ and 800 s, the slope according to the constant-thickness model matches reasonably well with that according to the diffusion model; the deviation is less than approximately 16%. For times $t > 800$ s deviations are larger and the constant-thickness model appears to be not valid anymore.

In both models, the constant thickness model and the diffusion model, the radial growth by entrainment is neglected, and slightly better results are expected when a correction for this growth is included. Therefore, an improvement of the present model would be one in which, of course, both the growth due to vertical diffusion and horizontal entrainment of ambient fluid are taken into account.

Nevertheless, one of the main conclusions that can be drawn from the present study is that the decay of planar dipolar vortex structures in a linearly stratified fluid is to a large extent governed by the diffusion of vertical vorticity.

ACKNOWLEDGMENT

One of us (JBF) gratefully acknowledges financial support by the Foundation for Fundamental Research on Matter (FOM) of the Netherlands Organization for Pure Research (NWO).

¹K. N. Fedorov and A. I. Ginsburg, "Mushroom-like currents (vortex dipoles): One of the most wide-spread forms of non-stationary coherent motions in the ocean," in *Mesoscale/Synoptic Coherent Structures in Geophysical Turbulence*, edited by J. C. J. Nihoul (Elsevier, Amsterdam, 1989), pp. 15–24.

²K. Ahlnäs, T. C. Royer, and T. M. George, "Multiple dipole eddies in the Alaska Coastal Current detected with Landsat Thematic Mapper data," *J. Geophys. Res.* **92**, 13041 (1987).

³J. C. McWilliams, "An application of equivalent modons to atmospheric blocking," *Dyn. Atmos. Oceans* **5**, 43 (1980).

⁴K. Haines and J. Marshall, "Eddy-forced coherent structures as a prototype of atmospheric blocking," *Q. J. Meteorol. Soc.* **113**, 681 (1987).

⁵Y. Couder and C. Basdevant, "Experimental and numerical study of vortex couples in two-dimensional flows," *J. Fluid Mech.* **173**, 225 (1986).

⁶J. M. NguyenDuc and J. Sommeria, "Experimental characterization of steady two-dimensional vortex couples," *J. Fluid Mech.* **192**, 175 (1988).

⁷G. R. Flierl, M. E. Stern, and J. A. Whitehead, "The physical significance of modons: Laboratory experiments and general integral constraints," *Dyn. Atmos. Oceans* **7**, 233 (1983).

⁸R. W. Griffiths and P. F. Linden, "The stability of vortices in a rotating, stratified fluid," *J. Fluid Mech.* **105**, 283 (1981).

⁹S. V. Fonseca, H. J. S. Fernando, and G. J. F. van Heijst, "The evolution of an isolated turbulent region in a stratified fluid," submitted to *J. Fluid Mech.*

¹⁰J. B. Flór and G. J. F. van Heijst, "An experimental study of dipolar vortex structures in a stratified fluid," *J. Fluid Mech.* **279**, 101 (1994).

¹¹G. J. F. van Heijst and J. B. Flór, "Dipole formation and collisions in a stratified fluid," *Nature* **340**, 212 (1989).

¹²S. I. Voropayev, Y. D. Afanasyev, and I. A. Filippov, "Horizontal jets and vortex dipoles in a stratified fluid," *J. Fluid Mech.* **227**, 543 (1991).

¹³V. V. Meleshko and G. J. F. van Heijst, "On Chaplygin's investigations of two-dimensional vortex structures in an inviscid fluid," *J. Fluid Mech.* **272**, 157 (1994).

¹⁴H. Lamb, *Hydrodynamics*, 6th ed. (Cambridge University Press, Cambridge, 1932).

¹⁵G. K. Batchelor, *An Introduction to Fluid Dynamics* (Cambridge University Press, Cambridge, 1967).

¹⁶J. J. Riley, R. W. Metcalfe, and M. A. Weissman, "Direct numerical simulations of homogeneous turbulence in density stratified fluids," *Proceedings of the AIP Conference of Nonlinear Properties of Internal Waves*, edited by B. J. West (American Institute of Physics, New York, 1981), pp. 79–112.

¹⁷G. E. Swaters, "Viscous modulation of the Lamb dipole vortex," *Phys. Fluids* **31**, 2745 (1988).

¹⁸S. Kida, M. Takoaka, and F. Hussain, "Formation of head–tail structure in a two-dimensional uniform straining flow," *Phys. Fluids A* **3**, 2688 (1991).

¹⁹H. J. Pearson and P. F. Linden, "The final stage of decay of turbulence in stably stratified fluid," *J. Fluid Mech.* **134**, 195 (1983).

²⁰J. M. H. Fortuin, "Theory and application of two supplementary methods of constructing density gradient columns," *J. Polym. Sci.* **44**, 505 (1960).

²¹H. Honji, S. Taneda, and M. Tatsuno, "Some practical details of the electrolytic precipitation method of flow visualization," *Rep. Res. Inst. Appl. Mech. Jpn.* **28**, 83 (1980).